Analyses of the effect of head imaging on medium demagnetization field in perpendicular recording

Hong Zhou[a)]
Seagate Research, 1251 Waterfront Place, Pittsburgh, Pennsylvania 15222-4215

Kaizhong Gao and H. Neal Bertram
CMRR 0401, UCSD, 9500 Gilman Drive, La Jolla, California 92093-0401

(Presented on 12 November 2002)

Poisson's equation is solved exactly to obtain the medium demagnetization field for both a single pole head and a single pole with a trailing shield (shielded single pole) head designs in perpendicular recording. To write an isolated transition, for the semi-infinite single pole head, head imaging can be neglected when calculating the demagnetization field. To the semi-infinite shielded single pole head, when the pole separation is reduced, perfect imaging from both the head and the soft magnetic underlayer is a good approximation. © *2003 American Institute of Physics.*
[DOI: 10.1063/1.1558186]

I. INTRODUCTION

Calculation of the medium demagnetization fields is essential to determine the transition parameter and the nonlinear transition shift in perpendicular recording.[1,2] Generally, the demagnetization field arises from the medium itself, but is altered by the permeabilities of both the soft magnetic underlayer (SUL) and the head. Fields from the medium and the SUL assuming perfect imaging can be easily calculated. The effect of head imaging on the demagnetization field was initially discussed in Ref. 3. However, the same issue was raised again recently in order to optimize head and medium designs.[4] A single pole head structure has been suggested for perpendicular recording. But to increase the writing field angle and gradient, a single pole including a trailing shield head design was also proposed.[5] In this article, Poisson's equation is solved exactly using a series expansion. The total demagnetization field of an isolated transition is then obtained.

Since the pole lengths are typically very large, in the following analyses, semi-infinite poles are assumed. The permeabilities of both the head and the SUL are set to be infinite. The written track width is also assumed infinite, thus only two-dimensional (2D) demagnetization fields are considered. An illustration of both head structures and coordinate systems is shown in Fig. 1. For the semi-infinite single pole head, a conformal mapping method has been applied to obtain the exact demagnetization field.[1] However, the implicit dependence on the recording geometry cannot be easily applied to calculate the field numerically. In addition, it is difficult to apply conformal mapping to a shielded head structure. It should be noted that CGS units are used.

II. SEMI-INFINITE SINGLE POLE HEAD

The coordinate system is shown in Fig. 1(a). The head-medium spacing is denoted as "d", the medium thickness is "t", and the medium-SUL separation is "s". In the following discussions, all lengths are scaled to the head-SUL spacing "L" ($L=d+t+s$). To solve Poisson's equation, the whole space is divided into two regions: I ($x<0$) and II ($x>0$).

A. Point charge $M_y(x_0,y_0)$ is located in region I

Using the Fourier analysis, the potential at each region can be written as (M_r is the media remanent magnetization):

$$\Phi_{\mathrm{I}}(x,y)/M_r=-\ln\left[\frac{(x-x_0)^2+(y-y_0)^2}{(x-x_0)^2+(y+y_0)^2}\right]+\int_0^\infty A(k)\sin(ky)e^{kx}dk,$$

$$\Phi_{\mathrm{II}}(x,y)/M_r=\sum_{m=1}^{\infty}B_m\sin(m\pi y)e^{-m\pi x}\ (0\leq y\leq 1). \quad (1)$$

The unknown parameters $A(k)$ and B_m are obtained from the boundary conditions at $x=0$:

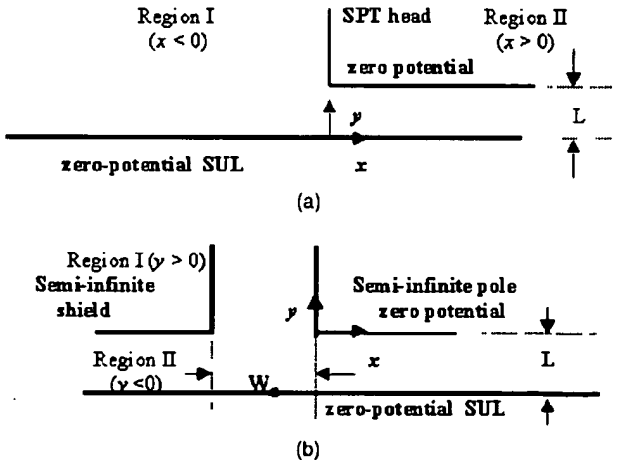

FIG. 1. Illustration of 2D head structures and coordinate systems: (a) Semi-infinite single pole head and (b) semi-infinite shielded single pole head. The pole separation in (b) is "W_g".

a)Electronic mail: hong.j.zhou@seagate.com

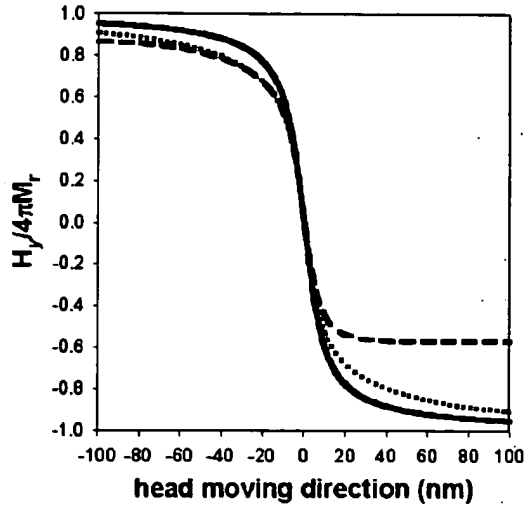

FIG. 2. Comparison of perpendicular demagnetization field calculations of an isolated transition for the semi-infinite single pole head (solid: Only medium self-demagnetization field; dashed: Medium field plus only SUL perfect imaging field; and dotted: Medium field plus both head and SUL imaging fields).

$$A(k)=\left\{\frac{1}{\pi}\sum_{m=1}^{\infty}B_m\left[\frac{\sin(k-m\pi)}{k-m\pi}-\frac{\sin(m\pi+k)}{m\pi+k}\right]\right\}-\frac{4}{k}e^{kx_0}\sin(ky_0),$$

$$B_m=-\frac{1}{m\pi}\left\{4x_0\int_0^1\left[\frac{1}{x_0^2+(y-y_0)^2}-\frac{1}{x_0^2+(y+y_0)^2}\right]\times\sin(m\pi y)dy+\int_0^{\infty}kA(k)\left[\frac{\sin(k-m\pi)}{k-m\pi}-\frac{\sin(m\pi+k)}{m\pi+k}\right]dk\right\}. \quad (2)$$

The solution of Eq. (2) requires the inversion of a truncated matrix. The fields at each region are

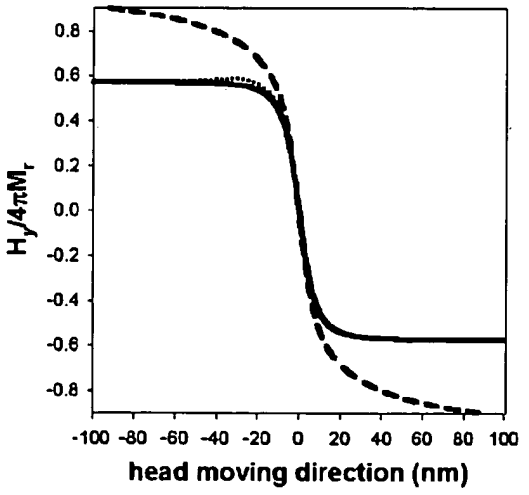

FIG. 3. Comparison of perpendicular demagnetization field calculations of an isolated transition for the semi-infinite shielded single pole head (dashed: Including only SUL perfect imaging field; solid: Including perfect imaging fields from both head and SUL, and dotted: Exact solution).

$$H_y^{(\mathrm{I})}(x,y;x_0,y_0)/(2M_r)=\left[\frac{y-y_0}{(x-x_0)^2+(y-y_0)^2}-\frac{y+y_0}{(x-x_0)^2+(y+y_0)^2}\right]+\left[\frac{y+y_0}{(x+x_0)^2+(y+y_0)^2}-\frac{y-y_0}{(x+x_0)^2+(y-y_0)^2}\right]-\sum_{m=1}^{\infty}B_m(x_0,y_0)m(-1)^m\int_0^{\infty}\frac{k\sin(m\pi k)}{k^2-1}\times\cos(m\pi ky)e^{m\pi kx}dk, \quad (3.1)$$

$$H_x^{(\mathrm{I})}(x,y;x_0,y_0)/(2M_r)=\left[\frac{x-x_0}{(x-x_0)^2+(y-y_0)^2}-\frac{x-x_0}{(x-x_0)^2+(y+y_0)^2}\right]+\left[\frac{x+x_0}{(x+x_0)^2+(y+y_0)^2}-\frac{x+x_0}{(x+x_0)^2+(y-y_0)^2}\right]-\sum_{m=1}^{\infty}B_m(x_0,y_0)m(-1)^m\times\int_0^{\infty}\frac{k\sin(m\pi k)}{k^2-1}\sin(m\pi ky)e^{m\pi kx}dk, \quad (3.2)$$

$$H_y^{(\mathrm{II})}(x,y;x_0,y_0)/M_r=-\sum_{m=1}^{\infty}m\pi B_m(x_0,y_0)\cos(m\pi y)e^{-m\pi x},$$

$$H_x^{(\mathrm{II})}(x,y;x_0,y_0)/M_r=-\sum_{m=1}^{\infty}m\pi B_m(x_0,y_0)\sin(m\pi y)e^{-m\pi x}, \quad (3.3)$$

$$H(x,y;y_0)=\int H(x,y;x_0,y_0)dx_0.$$

B. Point charge $M_y(x_0,y_0)$ is located in region II

In this case, the potentials are

$$\Phi_{\mathrm{I}}(x,y)/M_r=\int_0^{\infty}A(k)\sin(ky)e^{kx}dk,$$

$$\Phi_{\mathrm{II}}(x,y)/M_r=-\ln\frac{\cosh(\pi(x-x_0))-\cos(\pi(y-y_0))}{\cosh(\pi(x-x_0))-\cos(\pi(y+y_0))}+\sum_{m=1}^{\infty}B_m\sin(m\pi y)e^{-m\pi x}(0<y<1). \quad (4)$$

III. SEMI-INFINITE SHIELDED SINGLE POLE HEAD

From Fig. 1(b), to better solve the Poisson's equation for this structure, the coordinate system is chosen differently. The zero point is set at the corner of the main pole. The space is divided into two regions: I ($y>0$) and II ($y<0$). Again, all lengths are scaled to L. For this case, the potentials are easy to write down:

$$\Phi_{\mathrm{I}}(x,y)/M_r=\sum_{m=1}^{\infty}A_m\sin\left(\frac{m\pi x}{W}\right)e^{-m\pi y/W}\quad(-W\leq x\leq 0),$$

$$\Phi_{\mathrm{I}}(x,y)=0\quad(x<-W,\ x>0), \quad (5)$$

$$\Phi_{II}(x,y)/M_r = -\ln\left[\frac{(x-x_0)^2+(y-y_0)^2}{(x-x_0)^2+(y+2+y_0)^2}\right]+\int_0^\infty (B(k)\sin kx + C(k)\cos(kx)\sinh(k(1+y))dk.$$

Parameters $B(k)$, $C(k)$, and A_m are obtained similarly. The fields in region II are

$$H_x^{(II)}/M_r = \pi\left[\frac{\sinh(\pi(x-x_0))}{\cosh(\pi(x-x_0))-\cos(\pi(y-y_0))}-\frac{\sinh(\pi(x-x_0))}{\cosh(\pi(x-x_0))-\cos(\pi(y+2+y_0))}\right]$$
$$+\frac{1}{W}\sum_{m=1} mA_m\int_0^\infty k\frac{\sinh(k(1+y)m\pi/W)}{\sinh(km\pi/W)}\frac{\sin(km\pi x/W)-(-1)^m\sin(km\pi(x+W)/W)}{k^2-1}dk, \quad (6.1)$$

$$H_y^{(II)}/M_r = \pi\left[\frac{\sin(\pi(y-y_0))}{\cosh(\pi(x-x_0))-\cos(\pi(y-y_0))}-\frac{\sin(\pi(y+2+y_0))}{\cosh(\pi(x-x_0))-\cos(\pi(y+2+y_0))}\right]$$
$$-\frac{1}{W}\sum_{m=1} mA_m\int_0^\infty k\frac{\cosh(k(1+y)m\pi/W)}{\sinh(km\pi/W)}\frac{\cos(km\pi x/W)-(-1)^m\cos(km\pi(x+W)/W)}{k^2-1}dk. \quad (6.2)$$

They show that the demagnetization fields are the perfect imaging fields from head and SUL plus higher-order corrections.

IV. DEMAGNETIZATION FIELD OF AN ISOLATED TRANSITION

To record an isolated transition, since the transition region is located very close to the head edge, the following perfectly sharp transition is assumed:

$$M_y(x) = -M_r(x<0), \quad M_y(x) = M_r(x>0). \quad (7)$$

If only the SUL perfect imaging field is included, the demagnetization fields at the medium center plane can be easily obtained:

$$H_x(x)/M_r = -2\ln\frac{x^2+(2s+3t/2)^2}{x^2+(2s+t/2)^2},$$

$$H_y(x)/M_r = -8\tan^{-1}\left(\frac{x}{t/2}\right)+4\tan^{-1}\left(\frac{x}{2s+t/2}\right)$$
$$-4\tan^{-1}\left(\frac{x}{2s+3t/2}\right). \quad (8)$$

In Fig. 2, for the semi-infinite single pole head, the perpendicular demagnetization fields are compared for three cases: Only medium self-demagnetization field, medium field plus only SUL perfect imaging field [Eq. (8)], and medium field plus both head and SUL imaging fields. Parameters $d=15$ nm, $t=15$ nm, and $s=5$ nm are used. As can be seen, in the writing region ($x<0$), the demagnetization field including the medium contribution and only SUL perfect imaging [Eq. (8)] is sufficiently accurate. Note that discrepancy exists due to calculation errors. Thus, for a semi-infinite single pole head, head imaging can be neglected when calculating the transition parameter of an isolated transition.[1] However, head imaging must be included in analyzing the nonlinear transition shift.[2]

For the semi-infinite shielded single pole head, assuming perfect imaging is the field at the medium center plane (all lengths are scaled to L):

$$H_y^{(II)}(x)/(2M_r) = -2\tan^{-1}\left[\frac{\sin(\pi t/2)}{e^{-\pi x}-\cos(\pi t/2)}\right]+2\tan^{-1}\left[\frac{\sin(\pi t/2)}{e^{\pi x}-\cos(\pi t/2)}\right]+\tan^{-1}\left[\frac{\sin(\pi(2s+t/2))}{e^{-\pi x}-\cos(\pi(2s+t/2))}\right]$$
$$-\tan^{-1}\left[\frac{\sin(\pi(2s+t/2))}{e^{\pi x}-\cos(\pi(2s+t/2))}\right]-\tan^{-1}\left[\frac{\sin(\pi(2s+3t/2))}{e^{-\pi x}-\cos(\pi(2s+3t/2))}\right]+\tan^{-1}\left[\frac{\sin(\pi(2s+3t/2))}{e^{\pi x}-\cos(\pi(2s+3t/2))}\right], \quad (9)$$

However, when $x<0$, $\tan^{-1}(y/x) = \pi-\tan^{-1}(y/|x|)$,

$$H_x^{(II)}(x)/(2M_r) = -\ln\frac{\cosh(\pi x)-\cos(\pi(2s+3t/2))}{\cosh(\pi x)-\cos(\pi(2s+t/2))}.$$

In Fig. 3, for $W_g=50$ nm, three perpendicular field components are also compared: Including only SUL perfect imaging field [Eq. (8)], perfect imaging fields from both head and SUL [Eq. (9)], and exact solution [Eq. (6)]. The results demonstrate that perfect imaging from both the head and the SUL is a good approximation.

[1] K. Nakamoto and H. N. Bertram, J. Magn. Soc. Jpn. 26, 79 (2002).
[2] K. Nakamoto and H. N. Bertram, IEEE Trans. Magn. 38, 2069 (2002).
[3] M. F. Beusekamp and J. H. Fluitman, IEEE Trans. Magn. 21, 1414 (1985).
[4] M. Williams, C. Rettner, K. Takano, and W. Weresin, IEEE Trans. Magn. 38, 1643 (2002).
[5] M. Mallary, A. Torabi, and M. Benakli, IEEE Trans. Magn. 38, 1719 (2002).